Journal of Computer-Aided Molecular Design **17:** 367–382, 2003.

Molecular model of the neural dopamine transporter

Aina Westrheim Ravna, Ingebrigt Sylte & Svein G. Dahl*
Department of Pharmacology, Institute of Medical Biology, University of Tromsø, N-9037 Tromsø, Norway

Received 20 November 2002; Accepted in revised form 1 April 2003

Key words: cocaine, 3-dimensional structure, dopamine transporter, molecular dynamics, Na^+/H^+ antiporter, neurotransmitter, reuptake, secondary transporter

Summary

The dopamine transporter (DAT) regulates the action of dopamine by reuptake of the neurotransmitter into presynaptic neurons, and is the main molecular target of amphetamines and cocaine. DAT and the Na^+/H^+ antiporter (NhaA) are secondary transporter proteins that carry small molecules across a cell membrane against a concentration gradient, using ion gradients as energy source. A 3-dimensional projection map of the *E. coli* NhaA has confirmed a topology of 12 membrane spanning domains, and was previously used to construct a 3-dimensional NhaA model with 12 trans-membrane α-helices (TMHs). The NhaA model, and site directed mutagenesis data on DAT, were used to construct a detailed 3-dimensional DAT model using interactive molecular graphics and empiric force field calculations. The model proposes a dopamine transport mechanism involving TMHs 1, 3, 4, 5, 7 and 11. Asp79, Tyr252 and Tyr274 were the primary cocaine binding residues. Binding of cocaine or its analogue, (−)-2β-carbomethoxy-3β-(4-fluorophenyl)tropane (CFT), seemed to lock the transporter in an inactive state, and thus inhibit dopamine transport. The present model may be used to design further experimental studies of the molecular structure and mechanisms of DAT and other secondary transporter proteins.

Introduction

The sodium:neurotransmitter symporter family (SNF), belongs to the secondary transporter group of membrane proteins (Figure 1), and includes transporters for dopamine, GABA, serotonin (5-HT), norepinephrine and several other neurotransmitters and hormones [1]. Functional and phylogenetic analysis has indicated that these belong to a 'carrier' group of transporters which are structurally different from ion channel proteins [2]. The detailed 3-dimensional molecular structure is not known for any secondary transporter protein, but their primary structures indicate 12 membrane spanning domains and intracellular localisation of the amino and carboxy terminals [1, 3–5]. The human dopamine transporter (DAT) is an integral membrane protein with 620 amino acids [6]. Detailed molecular models of DAT [7], the serotonin transporter (5HTT) [8], Na^+/H^+ antiporter (NhaA) [9] and of two different glucose transporters, GLUT1 [10] and GLUT3 [11] have previously been proposed.

DAT terminates the action of dopamine by reuptake of the neurotransmitter into presynaptic neurons, and plays a key role in neuronal dopamine recycling [12]. The reuptake mechanism is Na^+ and Cl^- dependent, and follows a sequence of events where one dopamine molecule or two sodium ions initially bind to the transporter protein, followed by binding of one chloride ion to the transporter [13]. The inwardly directed sodium gradient provides energy for an inward movement of dopamine against a concentration gradient. DAT is the main molecular target of various psychomotor stimulants, including amphetamines and cocaine (Figure 2). The rewarding and reinforcing properties of cocaine are largely due to its inhibition of the DAT on terminals of mesolimbic-mesocortical dopaminergic neurons [12].

As indicated in Figure 1, the group of secondary transporter proteins also includes NhaA. An electron density projection map of the *Escherichia coli* NhaA

*To whom correspondence should be addressed. E-mail: sgd@fagmed.uit.no

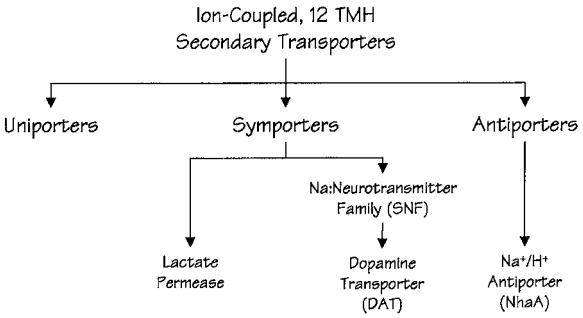

Figure 1. Secondary transporter families.

[14] confirmed a topology with 12 membrane spanning domains, and was used to construct a detailed molecular model of the NhaA [9].

Manual sequence alignment of the *E. coli* NhaA with the DAT, human 5HTT and human norepinephrine transporter (NET) (Figure 3), showed 7% identity and 22% similarity between the DAT and NhaA sequences. Similar alignment of the *E. coli* lactose permease symporter (lac permease) sequence showed 5% identity and 19% similarity with the DAT sequence (Figure 3). As demonstrated by bacteriorhodopsin and mammalian G-protein coupled receptors, which all have a common 7-TMH (transmembrane α-helix) folding motif, different proteins with a relatively low sequence similarity may still belong to the same folding family. Recent studies of the interactions of lysine and cysteine residues with extracellular agents support a previously proposed 12 TMH topology for 5HTT [5]. These results, together with the electron density projection map of NhaA [14] and a detailed topology analysis of NhaA [3], all support the assumption that the secondary transporter proteins have a 12 TMH folding motif in common.

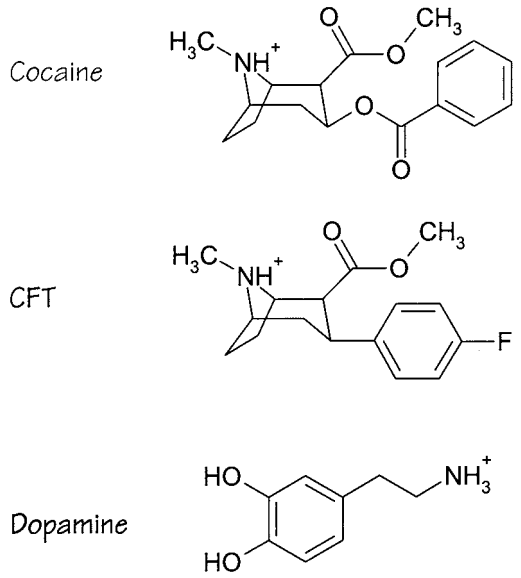

Figure 2. Molecular structure of cocaine, CFT ((−)-2β-carbomethoxy-3β-(4-fluorophenyl)tropane) and dopamine.

The present work was therefore based on the hypothesis that the *E. coli* NhaA, the *E. coli* lac permease and the mammalian sodium:neurotransmitter transporter family belong to a common folding class with 12 membrane spanning α-helices and intracellular localisation of the N- and C-terminals. The electron density projection map of the *Escherichia coli* NhaA [14], and results from site directed mutagenesis studies on DAT and 5HTT, were used to construct a detailed 3-dimensional DAT model. Cocaine and its analogue, (−)-2β-carbomethoxy-3β-(4-fluorophenyl)tropane (CFT) (Figure 2), were docked into a putative ligand binding area, in order to investigate hypothetical binding modes and identify interacting amino acids. Knowledge about the three-dimensional structure and molecular interactions between DAT and the ligands, cocaine and CFT, is important in order to understand the molecular mechanisms of the central nervous action of psychostimulants. Structural information regarding the binding site might be useful in the design of blockers of cocaine binding which are devoid of dopamine reuptake blocking activity.

Methods

Modelling of ligand molecules

Co-ordinates for cocaine and CFT were derived from the crystal structure of free cocaine base [15]. A hydrogen atom was added at the nitrogen atom in the model, in order to model the ionic form of the two ligands. Gaussian 94 [16] was used to calculate restrained electrostatic point (RESP) charges for cocaine, CFT and dopamine, using a RHF/6-31G* basis set. Molecular mechanics parameters that not were supplied with the AMBER force field, were chosen by analogy to the C-OH bond (tyrosine), the CT-CT-CT angle, the CT-C-O2 angle (carbonyl oxygen), the O-C-O angle (amino acid terminal residues), the CA-C-OH angle (tyrosine), the CB-C-O angle and the X-C-OH-X torsion angle (tyrosine) [17]. Parameters for the fluorine atom were taken from previous molecular modelling studies on ketanserin [18], and the

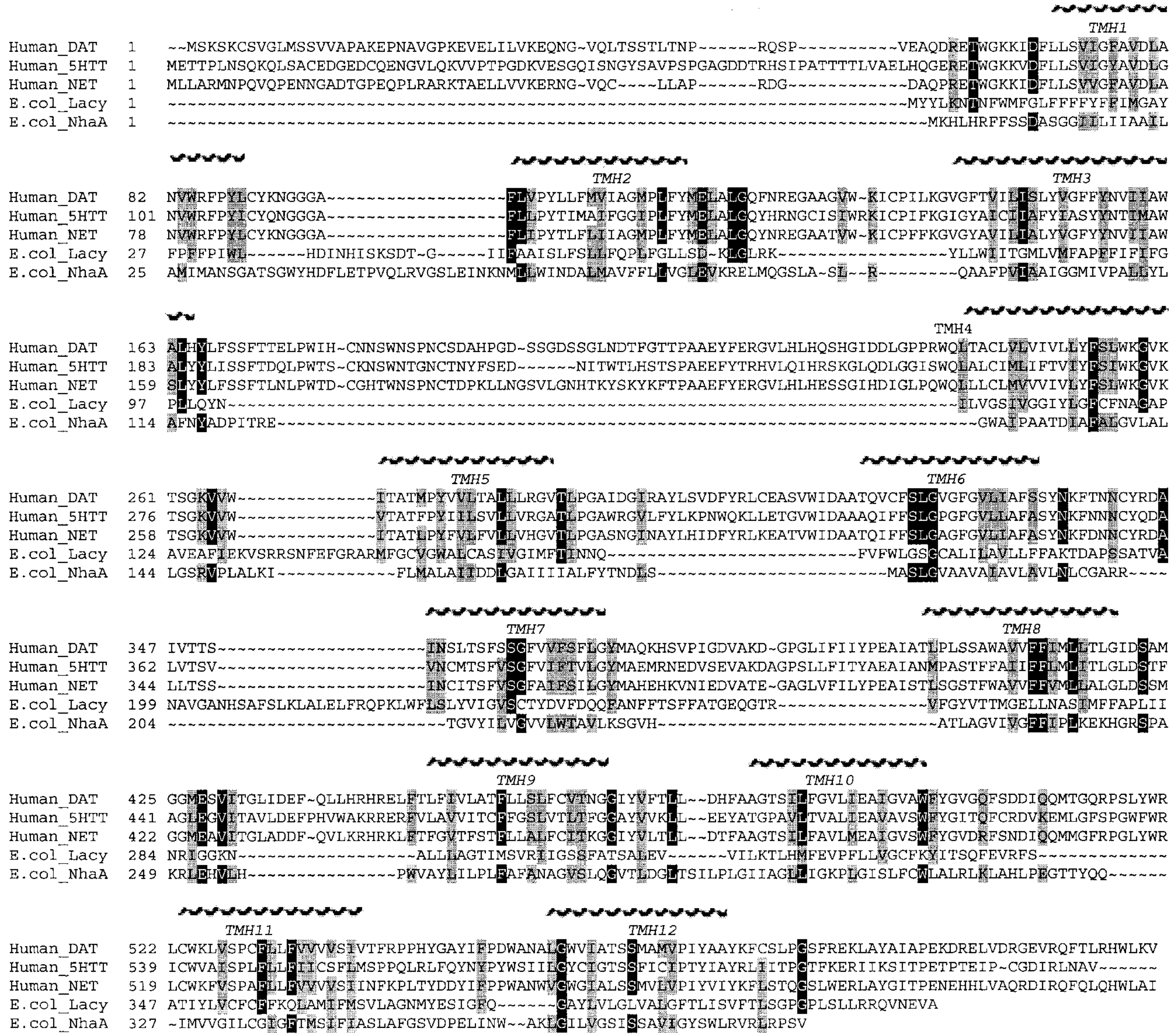

Figure 3. Sequence alignment of the human dopamine transporter (DAT), 5-HT transporter (5HTT) and norepinephrine transporter (NET), with the *E. coli* lac permease (Lacy) and NhaA antiporter. Alignment of DAT, 5HTT and NET was done with the ClustalW program [78]. NhaA and Lacy sequences were added by manual alignment.

parameters for the C-OS-CT angle were derived from a molecular modelling study of phospholipid surfaces [19]. Co-ordinates for the dopamine molecule were obtained from its crystal structure [20]. Parameters for dopamine that were not supplied with the AMBER force field, were chosen by analogy to tyrosine parameters [17].

Computational procedures

Interactive three-dimensional molecular graphics was done using the MIDAS plus software [21], and molecular mechanics and molecular dynamics (MD) calculations were performed with the AMBER 5.0 force field [22]. Molecular mechanics and MD calculations were performed with a distance dependent dielectric function ($\varepsilon = 4r_{ij}$), where r_{ij} is the interatomic distance between atoms i and j, and a 15 Å cut-off radius. Water molecules were not included in the calculations in order to limit the computing time. However, it has been shown that a dielectric constant of 4 and a distance dependent dielectric function of $\varepsilon = 4r_{ij}$ may reproduce the X-ray crystal structures of soluble proteins satisfactorily without including water molecules [23]. Energy minimisations were performed by 500 cycles of steepest descent minimisation followed by conjugate gradient minimisation until convergence. A convergence criterion of 0.0001 for the norm of the energy gradient was used for the ligands, and 0.02 for DAT and the transporter-ligand complexes. In order to increase the strength of the hydrogen bonds in the helices during MD simulations, backbone C-N intramolecular helical interactions were restrained with a constant of 5.0 kcal/mol and R_{eq} 3.1 Å, excluding proline residues. These restraint forces contribute to preserving of the helical conformation of TMHs during the MD simulations. A similar strategy for constraining the transmembrane helices, together with a dielectric constant of $\varepsilon = 4r$ and a distance dependent dielectric function, has previously been used during MD of membrane proteins [24, 25]. The DAT structure was subjected to 30 ps of MD with 'gradual heating' (0–300 K) followed by 150 ps of MD at 300 K. The CARNAL module of the AMBER program package was used to calculate the average structure from co-ordinates sampled each ps during the last 50 ps of the MD simulation. The transporter-ligand complexes were only subjected to 30 ps of MD with 'gradual heating' from 0 K to 300 K.

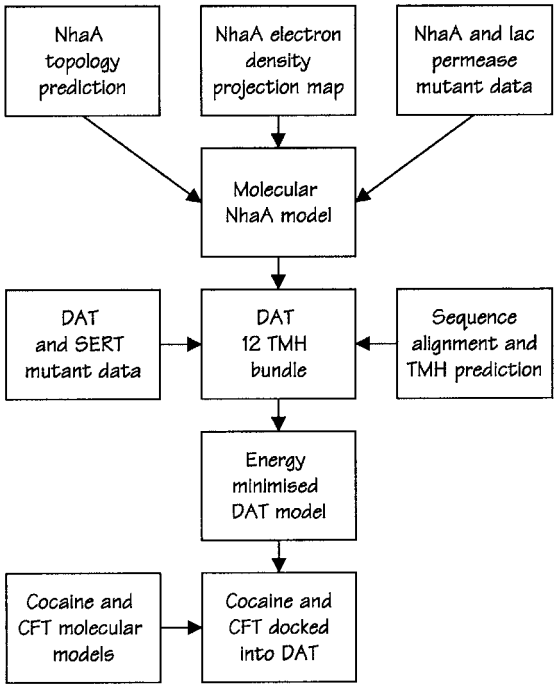

Figure 4. Procedure for construction of the DAT model and ligand docking.

Construction and refinement of the DAT model

The modelling procedure is indicated in Figure 4. The DAT model was based on TMH predictions, loop search in the PDB database [26], a previous molecular model of NhaA [9], and studies of ligand binding to mutated DAT and 5HTT [27–40].

The amino acid sequence of the human DAT (Swiss-Prot accession number Q01959) [6, 41] was submitted to the PredictProtein server [42] to obtain a multiple sequence alignment of the SNF proteins and a prediction of TMH regions.

The PredictProtein server was initially used to predict start and end points of each TMH of the DAT, but was only able to predict TMHs 2-12 and not the relatively hydrophilic TMH1. The start and end points of TMH1 was therefore taken from the Swiss-Prot database. Start and end residues of all TMHs are shown in Table 1. The 12 TMHs were individually built as α-helices using the MIDAS plus program [21].

The helical assembly of DAT was constructed using an approach similar to that in our previous model of NhaA [9]. The NhaA model was based on the electron density projection map of NhaA [14], a topology prediction of the antiporter [3], and data from site directed mutagenesis studies of NhaA in *E. coli* and

Table 1. Start and end points of TMHs 2-12 predicted by the PHD protein prediction server [42], and of TMH1 predicted by the Swiss-Prot amino acid sequence database, release 38 [41] for the human DAT (accession number Q01959).

TMH number	Amino acid sequence positions
1	69-89
2	98-115
3	141-165
4	240-257
5	268-285
6	316-333
7	352-369
8	400-419
9	450-467
10	480-497
11	523-541
12	560-577

Vibrio parahaemolyticus [43–49] (Table 2) and of lac permease of *E. coli* [4] (Table 3). The electron density projection map of NhaA did not indicate the order of the helices in the protein sequence, nor which side of the projection map that represents the periplasmic or cytoplasmic sides.

In agreement with the experimental constraints that TMH5 and TMH8 [4], and also TMH4 and TMH11 [49] (Table 2), should be adjacent to each other, and with the arrangement of TMHs 7, 8, 9, 10, and 11 suggested by Kaback (1997) (Table 3), these TMHs were subsequently arranged as in our previous NhaA model [9]. TMH12 was placed near TMH11, and the localisation of TMH6 accounted for the relatively short cytoplasmic loop between TMH6 and TMH7, tilted towards each other on the cytoplasmic side. TMHs 1, 2 and 3 were arranged using site directed mutagenesis data on dopamine and serotonin transporters as guidelines [29, 32, 33] (Table 4).

Studies of structure-function relationships of cocaine analogues have indicated the involvement of several polar residues and at least one hydrophobic residue in a cocaine interaction site on the DAT [12, 50]. Table 5 shows the amino acids assumed to be directly involved ligand binding, based on data from several ligand binding studies on mutated DAT and 5HTT [27–40]. These residues are localised in TMHs 1, 3, 4, 5 and 11, which were rotated along their helical axis such that a putative cocaine binding site was formed.

The putative cocaine interaction site included Phe76 [27] and Asp79 [29] (TMH1), Val152 [33, 38] and Tyr156 [33] (TMH3), Tyr252 [31] (TMH4), Tyr274 [31] (TMH5) and Phe534 [34] (TMH11). TMH7 was oriented such that serine residues appearing to be involved in dopamine transport were forming a putative dopamine translocation area [29, 30]. As indicated by site directed mutagenesis studies on DAT and its interactions with dopamine and MPP^+, a translocation area of DAT seems to include residues Asp79 (TMH1) [29], Ser357 and Ser360 (TMH7) [29], Ser351 and Ser354 (TMH7) [30], and Ser528, Ser539 and Phe534 (TMH11) [30]. Site directed mutagenesis studies have also indicated that several phenylalanine and proline residues are important for transporter function of the DAT. However, these residues are randomly distributed among the TMHs, located too far from each other and from Asp79 to form a distinct cocaine binding site, and are therefore most likely important for maintaining a proper transporter structure. The remaining TMHs were oriented with their polar residues pointing towards a central pore area representing a putative aqueous translocation pathway. All TMHs lining the pore were oriented such that hydrophilic residues were directed towards the putative translocation pathway, and hydrophobic residues were mainly oriented towards the membrane or other TMHs. Inter-helical van der Waals contacts were taken into account for each helix-helix interaction by orienting hydrophilic areas of the TMHs towards each other.

The putative ligand binding area of cocaine and CFT was studied by docking the cocaine molecule into the DAT model. Interactions between TMH3 and the ligand, as suggested by several studies, were difficult to obtain with the proposed helix arrangement in NhaA [9]. In order to obtain a molecular model in agreement with site directed mutagenesis data of 5HTT and DAT interactions with cocaine and CFT, the positions of TMH2 and TMH3 were interchanged from those in the NhaA model, such that the cocaine binding site was formed by side chains of TMHs 1, 3, 4, 5, 11. The helical arrangement of TMHs 1, 2 and 3 was considered as the most uncertain part of the NhaA model [9].

The side chains of the 12 TMH bundle were energy refined by 2500 steps of energy minimisation, followed by 50 ps of MD simulation at 300 K. Initial backbone conformations of loops between helices were constructed by searching for loop segments in the PDB database [26] using the FASTA program [51].

Table 2. Amino acids in NhaA suggested from site directed mutagenesis studies to be involved in transporter function.

Residue	Segment	Function	Reference
Val70, Phe71, Phe72, Leu73	TMH2	Amiloride sensitivity	[43]
Leu73	TMH2	pH sensing	[44]
Asp133	TMH4	Cation binding and transport	[45]
Asp133, Leu138	TMH4	Antiporter activity	[44]
Asp163, Asp164	TMH5	Cation binding and transport	[45]
His225	Cell exterior	pH sensing	[46], [48], [44]
Gly338	TMH11	pH response	[49]
	IC4	pH-induced conformational change	[47]

Table 3. Information on helix packing of lac permease from site directed mutagenesis studies [4].

Assumption	Based on
TMH5 and TMH8 adjacent	Involvement in substrate binding (Cys scanning)
Arrangement of TMHs 7, 8, 9, 10 and 11	Interacting amino acid pairs
TMH5 close to TMHs 7 and 8	Site directed spin labelling and thiol crosslinking experiments
Close proximity between TMH8 and TMH11	Monoclonal antibody study
TMH1 is close to TMH5 and TMH7	Site-directed crosslinking
TMH6 is close to TMH5 and TMH8	Site-directed crosslinking
Ligand binding causes translational or scissors-like movement of TMH7 and TMH2	Site-directed crosslinking
TMH7 in close proximity to TMHs 1, 2 and 11	Site-directed crosslinking

The loop conformations in the database having highest amino acid sequence homology with each of the loops of DAT were inspected visually, and the loop conformations having most reasonable steric interactions with the surrounding transporter segments, and smallest structural deviation from the terminal ends of the TMHs, were selected. Initial structures of the loops were constructed by replacing the side chains of the selected loop segments from the PDB database with the corresponding side chain in DAT.

No analogues for the entire N- and C-terminal, intracellular loop (IC) 1 or extracellular loop (EC) 2 were found in the PDB database. Initial models of these segments were constructed using a combination of secondary structure predictions by the PredictProtein server [42], and loop segments found in the PDB database. Due to their lengths, the terminals and loops had to be constructed from several fragments. Segments predicted by the PredictProtein server to be α-helices or β-sheets were modeled using MidasPlus, and known structural motifs for segments between these were obtained from the PDB database. His193, His375 and Glu396 of EC2 and EC4 were oriented towards each other in order to create the putative Zn^{2+} binding site suggested by Loland *et al.* [52].

Refinement of the loops was performed with 2500 steps of conjugate gradient minimisation with restraints on the TMHs, followed by 50 ps of MD at 300 K. The entire structure then was energy minimised and subjected to 30 ps of MD with 'gradual heating' (0–300 K) followed by 150 ps of MD at 300 K. The residues involved in a putative Zn^{2+} binding site [52] were restrained during the calculations, with a restraint constant of 28.0 kcal/mol and $R_{eq} = 2.0$ Å. The GRASP program [53] was used to calculate and visualise the electrostatic potential surface of DAT. Default values for the Poisson Boltzmann parameters were used; water probe radius 1.4 Å, interior and exterior dielectric constants 2.0 and 80.0, respectively [54]. Ionic radius: 2.0 Å

Docking and molecular dynamics simulation of DAT-ligand interactions

The cocaine and CFT structures were manually docked into the DAT model in 5 different orientations, using results from site directed mutagenesis studies (Table 4) as guidelines, and Asp79 in TMH1 as anchoring point for the protonated nitrogen atom of the ligand. The tree positions of each ligand with van der Waals contacts that best reproduced the site-directed mutagenesis data, were selected and energy minimised. MD simulations with gradual heating from 0 K to 300 K during 30 ps were performed on each of the 6 complexes, one simulation with restraints between the ligand and residues Asp79, Tyr256 and Tyr274, and one without such restraints, resulting in 12 different ligand-DAT complexes. Restraint constants: 10.0 kcal/mol for the ionic interaction and 8.0 kcal/mol for hydrogen bonds. Corresponding R_{eq} values: 2.0 Å and 2.6 Å. No conformational restraints were applied to the ligands during the simulations, in order to allow target-induced conformational changes, but only minor conformational changes of the ligands were observed.

After energy minimisation, the ligand-DAT interaction energy was calculated for each of the 12 complexes (Table 5). Restraints applied during the MD simulations were not included in the interaction energy calculations.

Since site directed mutagenesis studies have indicated that dopamine is translocated through DAT via serine residues on TMH7, a hypothetical translocation pathway was examined interactively by moving dopamine through the DAT model along TMHs 1, 4, 7 and 11.

Results

The arrangement of the 12 TMHs in the average co-ordinate set of the DAT model observed between 130 ps and 180 ps of MD simulations is shown in Figure 5A. TMHs 1, 2, 3, 4, 5, 7, 8, 11 and 12 formed a pore area that may represent a substrate translocation pathway. It is possible, therefore, that ligands inhibit dopamine transport by binding to this area.

Figure 5 also shows the water accessible surface and electrostatic potential field of the DAT model after MD simulation and energy refinement. As illustrated in Figure 5, the electrostatic potential distribution was dipolar, with the extracellular side mainly negative and the cytoplasmic side mainly positive. After MD simulations TMHs 1, 3 and 10 had tilted slightly and moved about 1 Å closer to the centre of the pore, which thus became narrower than before the MD. TMH5 was also slightly more tilted after the MD simulation. Since the pore area was narrower after the MD simulation, ligands could not be docked into the MD refined structure. This may have been due to the lack of water molecules in the pore area during the simulations, or that the simulations produced an inactive conformation of the transporter.

The loops moved towards each other and blocked the putative translocation area on the cytoplasmic side during the MD simulation. The C-terminal and the N-terminal were localised centrally over the helical bundle, further into the intracellular area than the loops between helices, and interacted with each other. IC1 and IC3 interacted with both the C-terminal and the N-terminal, while IC5 interacted with the C-terminal, IC3 and IC4. IC2 interacted with the C-terminal and IC1. IC4 moved slightly into the putative membrane area during the MD simulation, and this movement was larger than the movements of the other loops.

The extracellular loops were also closer to each other after the MD simulations. This was not surprising since restraints had been included in a putative Zn^{2+} binding area consisting of residues His193 (EC2), His375 and Glu396 (EC4). The average interatomic distance between the α-carbon atoms of these residues was 3 Å. EC2 created a lid covering the pore area when interacting with EC4. EC1 and EC6 interacted with EC2, EC3 interacted with EC4, and EC5 interacted with both EC2 and EC4 during the simulations.

Figure 6 shows the cocaine-DAT and CFT-DAT complexes after energy refinement, and interaction energies of the complexes between DAT and cocaine/CFT are given in Table 5. After energy minimisation of cocaine in 3 different positions in DAT using Asp79 in TMH1 as an anchoring point, strongest interactions, besides the ionic Asp – N^+ interaction, were observed between the ester moieties of the ligand and Tyr252 (TMH4) and Tyr274 (TMH5).

Both ester moieties of the cocaine molecule formed hydrogen bond interactions with either of the two tyrosine residues, depending on the ligand orientation. In one position, the benzoate ester of cocaine formed a hydrogen bond with Tyr252 and the methanol ester formed a hydrogen bond with Tyr274. When the cocaine molecule was rotated 180 degrees, these hydrogen bond interactions were inverted. When

Table 4. Transporter protein residues involved in binding of cocaine and CFT. hDAT: human DAT; rDAT: rat DAT; bDAT: bovine DAT.

TMH	Transporter	Residue	Corresponding hDAT residue	Reference
1	rDAT	Phe76	Phe76	[27]
1	rDAT	Asp79	Asp79	[29]
3	5HTT	Ile172	Val152	[33]
		Tyr176	Tyr156	
3	bDAT	Val152	Val152	[38]
4	rDAT	Tyr251	Tyr252	[31]
5	rDAT	Tyr273	Tyr274	[31]
11	rDAT	Tyr533	Phe534	[34]

Table 5. Relative ligand-DAT interaction energies after MD simulation and energy minimisation

Ligand	Complex number[a]	Applied restraint during heating	Relative interaction energy[b] (kcal/mol)
Cocaine	1		−0.4
Cocaine	1	X	−5.0
Cocaine	2		0
Cocaine	2	X	−11.7
Cocaine	3		−0.9
Cocaine	3	X	−5.7
CFT	4		−8.7
CFT	4	X	−7.6
CFT	5		0
CFT	5	X	−0.7
CFT	6		−4.1
CFT	6	X	−6.4

[a]Number indicates starting position of the ligand before energy minimisation.
[b]Relative to the complex with weakest interaction for each ligand.

cocaine was kept unrestrained during the MD simulations, the ligand either stayed in the docked position or lost contact with one of the tyrosine residues, with the benzene moiety oriented towards the cytoplasmic region or the extracellular region.

During the simulations with unrestrained CFT the ligand lost contact with either Tyr252 or Tyr274, depending on the initial position. The ester group of CFT remained in contact with Tyr252 or Tyr274, while the benzene moiety was oriented towards the cytoplasm or periplasm, or stayed in the initial position.

The hydrophobic residues, Phe76, Leu80, Val83 (TMH1), Phe154 and Phe155 (TMH3), Val245, Ile248 and Val249 (TMH4), Leu277 (TMH5), and Phe531 and Phe534 (TMH11) lined the cocaine/CFT binding site. Hydrophobic residues on TMHs 1, 3 and 4 interacted with the tropane ring of the ligands and hydrophobic residues on TMH5 and TMH11 interacted with the benzene moiety. The hydrophobic residues contributing to the binding site were somewhat dependent on the initial docking position of the ligand. The ligands interacted with Ser357 and Ser360 (TMH7), as well as with Tyr151 (TMH3). TMH2 and TMH12 had less contact with the pore area than the other TMHs.

Dopamine was docked into three different putative translocation pathway positions (Figure 7), near the periplasmic side (A), centrally (B), and near the cytoplasmic side (C), and seemed to be able to transverse DAT along TMH7 while interacting with TMHs 1, 4, 5, 11, and possibly also TMH3. Interestingly, the docking of dopamine in position B (Figure 7) permitted direct interactions between its positively charged nitrogen atom and Asp79 (TMH1), and between the two hydroxyl groups of dopamine and Ser357 and

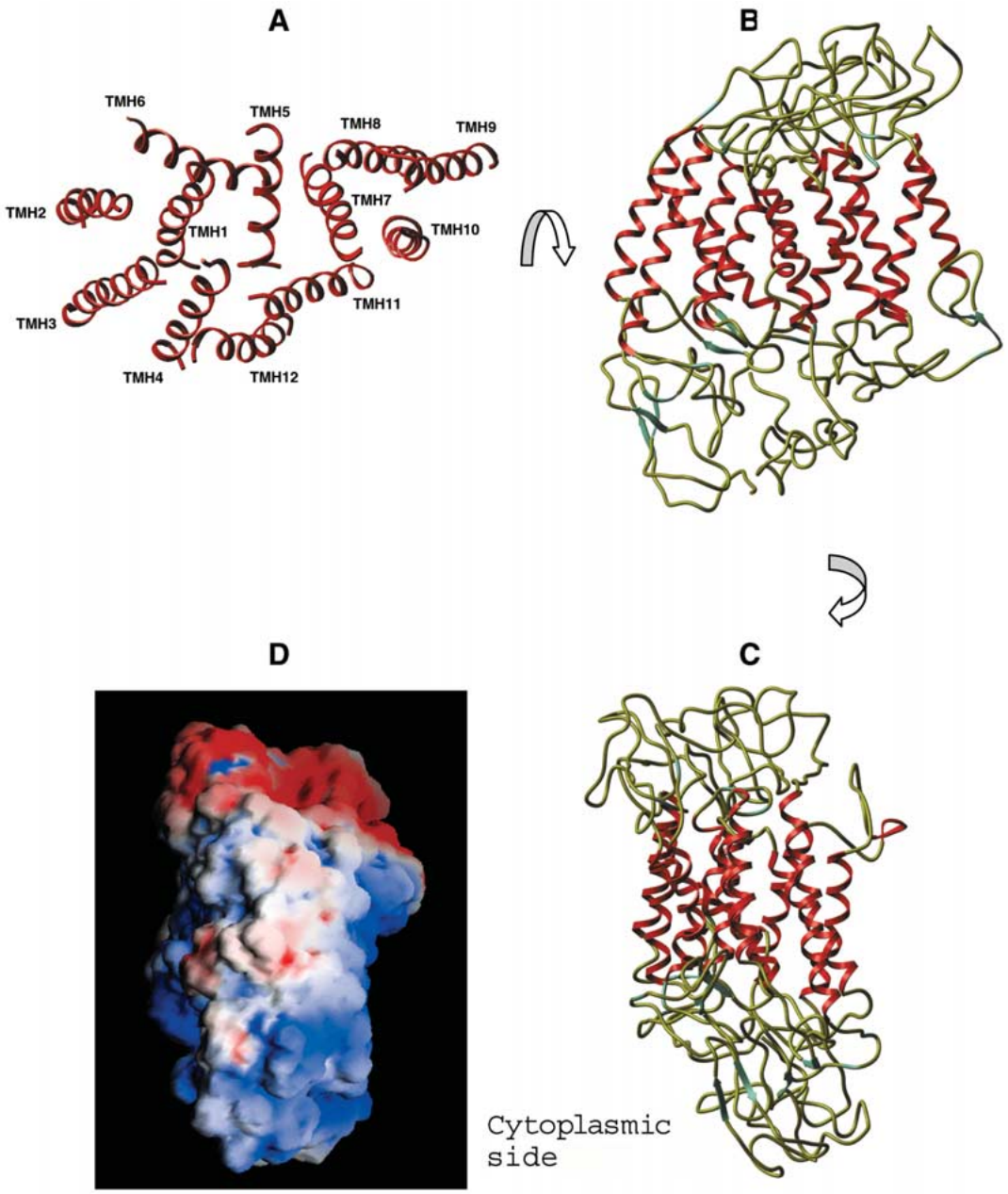

Figure 5. Energy refined DAT model. A: Backbone structure of the TMHs, viewed from the extracellular side. B and C: Backbone structure of the entire model, viewed in the membrane plane. D: water accessible surface, coloured according to electrostatic potentials: negative – red, positive – blue, viewed in the same projection as C.

Ser360 (TMH7). This is in accordance with suggestions by Kitayama *et al.* [29] of possible interactions during dopamine translocation through the transporter. Position A (Figure 7) led to interactions with Phe534 (TMH11) and Asp79, and position C led to interactions with Ser354 and Ser351 (TMH7) and Tyr252 (TMH4). TMH5 seemed to sterically hinder this translocation of dopamine in a rigid DAT model, and would have to move from its present position in the model during the translocation process.

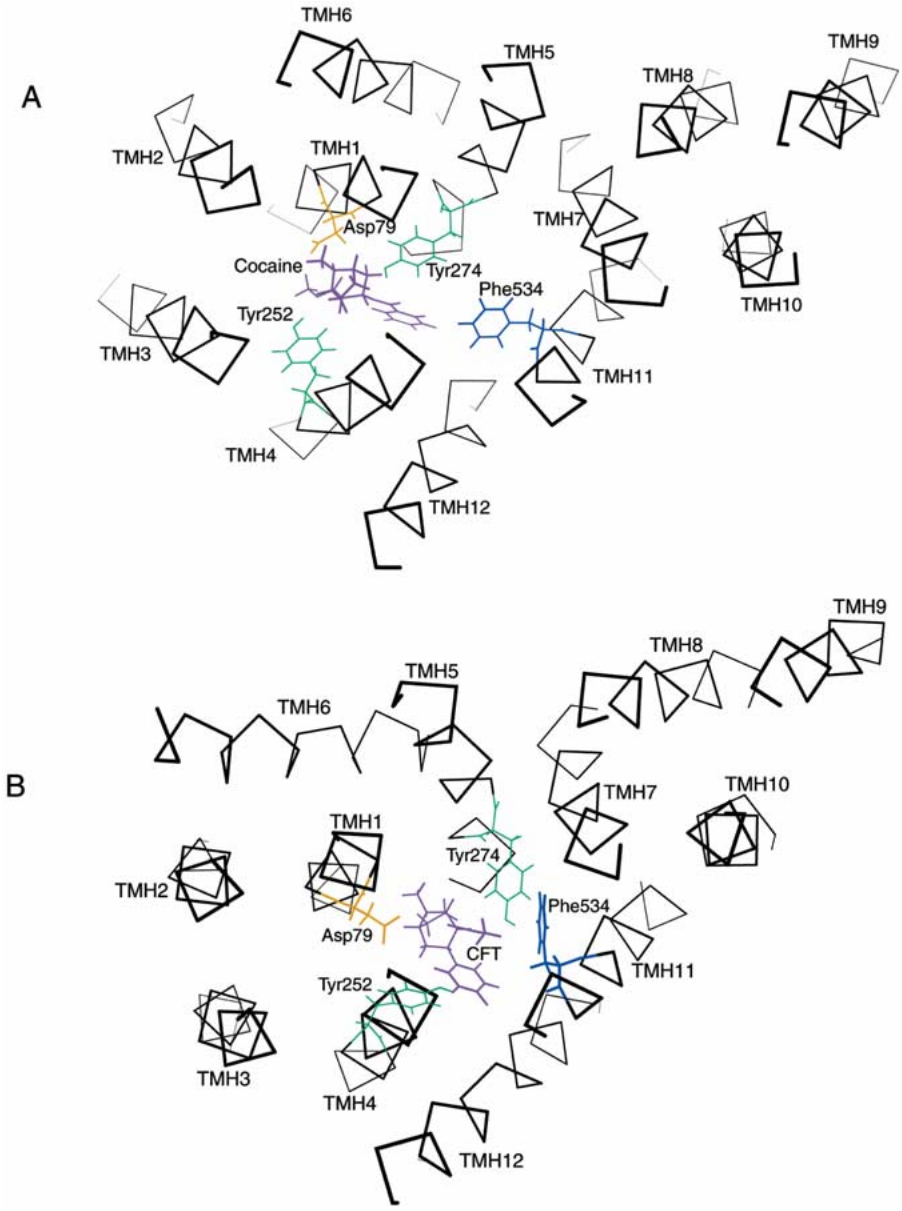

Figure 6. Cα traces of the TMHs, viewed from the extracellular side, with cocaine (A) and with CFT (B) in the binding pocket. Residues with strongest ligand interactions: Asp79: orange, Tyr252: green, Tyr274: green and Phe534: blue.

Discussion

Traditional homology modelling of proteins use x-ray structures of structurally related proteins as templates. For secondary transporter proteins, no such template is available. An x-ray structure of the *E. coli* MsbA, which belongs to the Multidrug Resistance ATP Binding Cassette (ABC) transporters, was recently published [55]. This protein is a homodimer with 6 TMHs in each subunit, using ATP as energy source. However, the MsbA structure was not considered as a suitable template for modelling of the dopamine transporter, which has a different functional mechanism.

The crystal structure of the bacterial multidrug efflux transporter, AcrB, has recently been reported [56]. AcrB is part of a bacterial resistance system and co-operates with a membrane fusion protein, AcrA, and an outer membrane channel, TolC. AcrB is or-

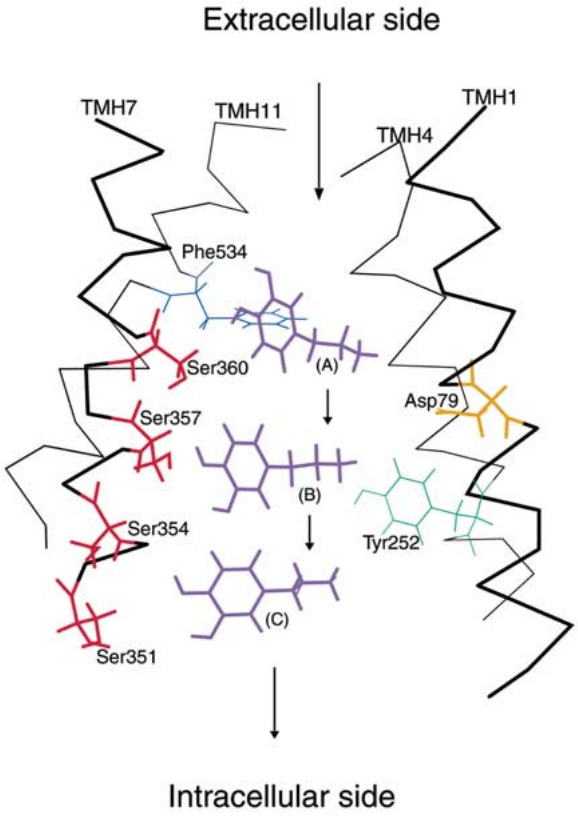

Figure 7. Putative dopamine translocation pathway. Side chains of residues that may be important for dopamine translocation are displayed. Colour coding: Ser351, Ser354, Ser357 and Ser360: red, Asp79: orange, Tyr252: green, Phe534: blue.

ganized as a homotrimer, each subunit containing 12 TMHs and two large hydrophilic loops on the periplasmic surface. The structure implies that substrates are translocated through a pore between the three AcrB subunits or through the center of each subunit. AcrB, which has a broad substrate specificity and extrudes cationic, neutral and anionic substances, is believed to be a proton antiporter and belongs to the RND (resistance-nodulation-cell division) transporter superfamily [57]. In the present study, the crystal structure of AcrB was not regarded as a suitable template for a DAT model, for the following reasons: The TMH arrangement of AcrB is not in agreement with site directed mutagenesis data on DAT and SERT since both TMH1 and TMH7 would be unable to take part in ligand binding, AcrB is part of an efflux system with low substrate specificity and interacting with other proteins as part of its mechanism, and no experimental studies have indicated a homotrimeric organization for the DAT.

A three dimensional structure of a bacterial oxalate transporter (OxlT), derived from analysis of two-dimensional crystals, has also recently been reported [58]. OxlT belongs to the major facilitator superfamily (MFS), and carries out a selective exchange of oxalate for formate across the inner membrane of *Oxalobacter formigenes*. The density map of OxlT does not permit direct assignment of the TMHs, and the TMH assignment proposed by the authors does not fit with site directed mutagenesis data on DAT and SERT. The OxlT structure was therefore not regarded as a suitable template for a DAT model.

NhaA is a Na^+/H^+ antiporter while DAT is a Na^+-neurotransmitter symporter (Figure 1), and their 3-dimensional structural resemblance remains to be established. However, due to their common functional mechanism, where an ion gradient is used as energy source for translocation of molecules against a concentration gradient, we propose the hypothesis that ion-coupled secondary transporters represent a common 12 TMH folding class. In this case, the NhaA currently provides the best available structural basis for molecular modelling of DAT and other secondary transporter proteins. As shown in the present study, the use of NhaA as a structural basis produced a putative ligand binding site of DAT that was in agreement with results from experimental ligand binding studies.

As in the previous NhaA model [9], the positioning of the TMHs in the membrane was based on the experimental NhaA electron density map, while allocation of each of the 12 postulated TMHs in the sequence to the putative α-helices in the electron density map was based on biological and biophysical data. Analysis the data summarised in Tables 2–4, including ligand binding to the DAT and 5HTT, indicated a different position of TMH2 and TMH3 than in the previous NhaA model. Although the positions of TMH2 and TMH3 in the present DAT model therefore seem most likely, this part of the model has to be further validated by experimental studies. The DAT model provides a tool for design of such studies.

Hydropathy plots of SNF protein sequences show a conserved region after the N-terminal, which has hydrophilic character and appears to be an amphipatic α-helix with several conserved polar residues localised to one side of the helical axis [1]. This sequence was assigned to TMH1 in the present model. Alternative topologies of SNF proteins have been proposed, where either TMH1 [59, 60] or TMH2 [61] does not span the membrane. An additional TMH between TMH3 and TMH4 has also been suggested [59–61]. However, re-

cent studies of the interactions of lysine and cysteine residues with extracellular agents support the originally proposed 12 TMH topology for the serotonin transporter [5].

The central pore of the DAT model, formed by TMHs 1, 3, 4, 5, 7, 8 and 11, is in accordance with studies of several other secondary transporters including GLUT1, which is assumed to have an aqueous pathway consisting of TMHs 3, 5, 7, 8 and 11 [62]. TMH1, which fails to be predicted by several theoretical methods for secondary structure prediction, does not have contact with the putative membrane area in the present DAT model, and is localised near the translocation pathway. Sequence similarity data indicate that TMH1 has unique properties, and it also shows the highest amino acid similarity (67%) of all the predicted TMHs among SNF proteins [63]. TMH1 therefore seems to be important for neurotransmitter recognition and/or transport.

During MD simulations of DAT, helical movements made the pore area narrower and the putative ligand-binding cavity became too narrow to accommodate the cocaine and CFT molecules. The NhaA projection map, which was the basis for the DAT model, was determined from 2-dimensional crystals at low pH, where NhaA is in an inactive state [14].

The helical orientations of the DAT model, relative to the inside/outside of the membrane, was based on those of our previous NhaA model [9], in which their orientation seen from the periplasmic side fits with the electron density map of NhaA [14]. In particular, a short loop between TMH6 and TMH7 on the cytoplasmic side, where these two TMHs are tilted towards each other, and a compact loop between TMH10 and TMH11, resembling the L-shaped structure in the NhaA electron density map, support the helical orientation in the NhaA model.

A putative Zn^{2+} binding site, proposed by Loland *et al.* [52], was included in the DAT model. Allosteric inhibition of the DAT by ligand interactions in this extracellular loop area may be possible. Ligands may interact with His193 of EC2 and His375 and Glu396 of EC4, in a position that may close the entrance to the translocation pathway.

Cocaine and CFT were docked into the putative ligand binding area of the DAT model before MD simulations. Presuming that this DAT conformation represents an inactive state of the transporter, binding of cocaine or CFT seemed to lock the transporter in the inactive state, and thus inhibit dopamine transport. This might be a molecular mechanism for the inhibition of neural dopamine reuptake by cocaine and CFT [29]. The cocaine binding area in the DAT model had residues contributing to ionic-, hydrophilic- and hydrophobic interactions with cocaine. In the model Asp79 (TMH1), Tyr252 (TMH4) and Tyr274 (TMH5) are part of a ligand binding area, where Asp79 interacts with the positively charged nitrogen atom of cocaine, and the two tyrosine residues with the two ester groups of cocaine. A hydrogen bond interaction between the benzoate carboxyl and the hydroxyl group of a tyrosine residue has been demonstrated in the crystal structure of a bacterial cocaine esterase [64]. It may not be ruled out, however, that the aromatic moieties of the tyrosines may interact via cation-π interaction with the protonated nitrogen atom in cocaine. A cation-π interaction may also be present between the protonated nitrogen and Phe76, which is localized one α-helical turn further towards the cytoplasm than Asp79 of TMH1. Cocaine and CFT may also interact by hydrogen bonds to Ser357 and Ser360, as dopamine does. According to the present model, this would require a slight conformational change in order to shorten the distance between TMH1 and TMH7. CFT has only one ester group and might be oriented slightly differently from cocaine in the binding area. CFT lost contact with either Tyr252 or Tyr274, depending on the initial position of the ligand, during MD simulations without restraints between the ligand and the DAT.

Several hydrophobic residues also interacted with cocaine and CFT, which both are relatively lipophilic. Site-directed mutagenesis studies of the cocaine binding site in 5HTT, using the high affinity fluorescent cocaine-analogue, RTI-233, have demonstrated that the cocaine interaction area is highly hydrophobic [65]. During MD of ligand-DAT complexes all ligands kept their ionic contact with Asp79, and the hydrophilic interactions were generally maintained. This indicates that Asp79, Tyr252 and Tyr274 are the primary cocaine binding residues, and that the ligands may undergo small movements among the hydrophobic residues during binding to the transporter. The role of the residues lining the putative cocaine binding area of the DAT model in cocaine and CFT binding may be examined by site directed mutagenesis studies. The 5HTT residue Met180 (TMH3), which corresponds to Ile160 in DAT, was suggested to be part of a citalopram binding pocket in a recent species scanning mutagenesis study on 5HTT [66]. In the present DAT model, this residue is close enough to the cocaine binding area to take part in binding.

The cocaine binding part of the DAT model was based on data from several site directed mutagenesis studies of cocaine and CFT interacting with DAT and 5HTT [27–40], and should be reasonably accurate. However, the interpretation of site directed mutagenesis data is not unambiguous, since observed effects of mutations on binding may be due to other structural changes than direct disruption of residue side chain-ligand interactions. Site directed mutagenesis studies have indicated that several phenylalanine and proline residues are important for DAT transporter function [27, 28]. The present DAT model suggests that these residues may be important for maintaining a proper protein structure, thus affecting ligand binding affinity indirectly, since most of these residues were too far from Asp79 to be able to form a cocaine binding site that also includes Asp79. Experimental studies have shown that mutation of cysteine residues in extra- and intracellular loops affect CFT binding to DAT [67], apparently by inducing conformational changes in the protein. Mutation of a tyrosine residue in the third intracellular loop of DAT decreased cocaine binding affinity, also most likely by an indirect mechanism [68]. The present model focused on a putative ligand binding area the transmembrane domain, using Asp79 as an anchoring point, and did not examine the possible role of the extra- and intracellular loops in cocaine binding.

The model may be used to design further site directed mutagenesis studies of the DAT. The relative importance of the physicochemical environment surrounding the cocaine binding area might be examined by mutating hydrophobic residues into hydrogen bond donors like serine, or into bulk amino acids contributing to steric hindrance of ligand interactions.

Interactions of dopamine with a putative translocation pathway in the DAT have been examined by experimental studies [29, 30]. The dopamine transport mechanism may involve several conformational changes in the transporter. As indicated by studies on lac permease, the 12 TMHs may be more loosely packed in an active state, with water in the cavities, and widespread co-operative conformational changes including sliding and tilting motions of the TMHs may occur during ion transport [4]. The present DAT model proposes a translocation pore formed by TMHs 1, 3, 4, 5, 7, and 11, where dopamine interacts with Phe534 (TMH11), Tyr252 (TMH4), Tyr274 (TMH5) and Asp79 (TMH1), and moves through a pore lined with serine residues in TMH7 (Ser360, Ser357, Ser354 and finally Ser351) before entering the cytoplasm (Figure 7), in agreement with previous experimental studies [29, 30].

The exchange-diffusion model of amphetamine-induced dopamine release through DAT [69, 70], and implications that 5HTT acts as a 5-HT/amphetamine exchange system [71], indicate that amphetamine may stimulate dopamine release into the extracellular side of DAT with the exchange taking place at the binding site [69]. It has been proposed that there may be two different ion translocation pathways through the NhaA transporter [14]. According to the present model, two different pathways of the DAT may be partly separated by TMH4 and TMH5 (Figure 5A). The intracellular loop (IC2) between these TMHs divides the pore area into two possible ion translocation regions, which might be involved during amphetamine-dopamine exchange.

IC4 of NhaA appears to be involved in pH-induced conformational changes leading to activation of the transporter [47]. The NhaA model suggested that conformational changes in IC4 is accompanied by alterations of the positions of TMHs 4, 5 and 11 relative to each other, such that a pore area of the transporter protein is opened [9]. IC4 is rich in charged amino acids, both in NhaA and in DAT, and is relatively well conserved within the SNF family. Conformational changes involving IC4 and the relative positions of TMH4, TMH5 and TMH11 may be involved in the dopamine transport mechanism. During MD simulations of the DAT model, IC4 changed conformation and moved slightly into the putative membrane area. However, it is possible that the conformational change of IC4 was due to the lack of stability of the initial structure of the model or to lack of solvation, and this observation could therefore be fortuitous.

Experimental studies have shown that the external loops of 5HTT are not substrate or inhibitor binding sites, but contribute to the stability and conformational flexibility of the transporter [39]. Similar results have been reported for residues in the cytoplasmic loops of the DAT [67, 72, 73]. The initial models of the N- and C-terminal domains containing 45 and 70 residues, and the intracellular and extracellular loops with up to 75 residues, were partly based on known structural motifs from the PDB database [26], but must still be considered as relatively crude approximations. In spite of this, the loops and terminals were included in order to get a more correct distribution of masses and electrostatics in the simulations than in a model of only the TMHs. Including the loops and terminals also enabled reconstruction of a previously proposed Zn^{2+}

binding site [52], but it should be kept in mind that the applied computational techniques for loop modeling were relatively inaccurate, and that these were the most uncertain parts of the model.

Due to the relatively low level of accuracy of the present DAT model, all calculations were done in vacuum. For the same reason, sophisticated solvation and/or membrane models was not warranted, although the omission of solvation and membrane molecules may have influenced its structure and dynamics. Calculations were performed with a distance dependent dielectric function ($\varepsilon = 4r$) in order to compensate for not including water molecules in the calculations.

Oligomerization of SNF proteins may be involved in their transport mechanisms [74–77], but it is not clear whether dimerisation or tetramerisation is essential for functional activity. In the electron density projection map of the *Escherichia coli* Na^+/H^+ antiporter dimer, the distance between the two monomers suggests that the translocation pathway is not at the dimer interface [14]. However, this electron density projection map may not present a biologically relevant monomer-monomer interaction.

Conclusions

Experimental studies of the topology of the 5-HT transporter [5], an electron density projection map of the NhaA [14], and a detailed topology analysis of NhaA [3], all support the assumption that these secondary transporter proteins have 12 membrane spanning domains and intracellular location of the N- and C-terminals. Based on the hypothesis that the membrane spanning domains are α-helices, and that secondary transporter proteins belong to a common folding class, we have constructed a 3-D model of the dopamine transporter from the NhaA projection map by computational modelling, and refined it by molecular mechanical energy minimisation and molecular dynamics simulations. In the model Asp79 (TMH1), Tyr252 (TMH4) and Tyr274 (TMH5) were the primary cocaine binding residues, and residues lining the cocaine binding area include Phe76, Leu80, Val83 (TMH1), Tyr151, Phe154, Phe 155 (TMH3), Val245, Ile248 and Val249 (TMH4), Leu277 (TMH5), Phe531, and Phe534 (TMH11). The model suggests that dopamine initially interact with Phe534 (TMH11), Tyr274 (TMH5) and Asp79 (TMH1), and move through a pore lined with serine residues in TMH7 (Ser360, Ser357, Ser354 and finally Ser351), before entering the cytoplasm.

The present DAT model was partly based on approximations, but may be used to select residues for further site directed mutagenesis studies that may be used to refine the DAT model.

Note

Co-ordinates of the DAT model are available from the authors upon request.

Acknowledgements

The present study was supported by computer time on the HP RISC supercomputer at the University of Tromsø, Norway.

References

1. Reizer, J., Reizer, A. and Saier, M.H., Jr., Biochim. Biophys. Acta, 1197 (1994) 133.
2. Saier, M.H., Jr., Microbiol Mol Biol Rev, 64 (2000) 354.
3. Rothman, A., Padan, E. and Schuldiner, S., J. Biol. Chem., 271 (1996) 32288.
4. Kaback, H.R. and Wu, J., Q. Rev. Biophys., 30 (1997) 333.
5. Chen, J.G., Liu-Chen, S. and Rudnick, G., J. Biol. Chem., 273 (1998) 12675.
6. Giros, B., el Mestikawy, S., Godinot, N., Zheng, K., Han, H., Yang-Feng, T. and Caron, M.G., Mol. Pharmacol., 42 (1992) 383.
7. Edvardsen, O. and Dahl, S.G., Brain Res. Mol. Brain. Res., 27 (1994) 265.
8. Ravna, A.W. and Edvardsen, O., J. Mol. Graph. Model., 20 (2001) 133.
9. Ravna, A.W., Sylte, I. and Dahl, S.G., Receptors and Channels, 7 (2001) 319.
10. Zeng, H., Parthasarathy, R., Rampal, A.L. and Jung, C.Y., Biophys. J., 70 (1996) 14.
11. Dwyer, D.S., Proteins, 42 (2001) 531.
12. Uhl, G., Lin, Z., Metzger, T. and Dar, D.E., Methods Enzymol., 296 (1998) 456.
13. Boja, J.W., Vaughan, R., Patel, A., Shaya, E.K. and Kuhar, M.J., In Boja, J.W., Vaughan, R., Patel, A., Shaya, E.K. and Kuhar, M.J. (Eds), Dopamine receptors and transporters, Marcel Dekker, New York, 1994, 611.
14. Williams, K.A., Nature, 403 (2000) 112.
15. Hrynchuk, R.J., Barton, R.J. and Robertson, B.E., Can. J. Chem., 61 (1983) 481.
16. Frisch, M.J., Trucks, G.W., Schlegel, H.B., Gill, W., Johnson, B.G., Robb, M.A., Cheeseman, J.R., Keith, T., Petersson, G.A., Montgomery, J.A., Raghavachari, K., Al-Laham, M.A., Zakrzewski, V.G., Ortiz, J.V., Foresman, J.B., Cioslowski, J., Stefanov, B.B., Nanayakkara, A., Challacombe, M., Peng, C.Y., Ayala, P.Y., Chen, W., Wong, M.W., Andre, J.L., Replogle, E.S., Gomperts, R., Martin, R.L., Fox, D.J.,

Binkley, J.S., Defrees, D.J., Baker, J., Stewart, J.P., Head-Gordon, M., Gonzales, C. and Pople, J.A., *Gaussian 94*, 1995, Gaussian Inc: Pittsburg PA.
17. Ravna, A.W., Schroder, K.E. and Edvardsen, O., Comput. Chem., 23 (1999) 435.
18. Kristiansen, K., Edvardsen, O. and Dahl, S.G., Med. Chem. Res., 3 (1993) 370.
19. Charifson, P.S., Hiskey, R.G. and Pedersen, L.G., J. Comput. Chem., 11 (1990) 1181.
20. Giesecke, J., Acta Crystallogr., B36 (1980) 178.
21. Ferrin, T.E., Huang, C.C., Jarvis, L.E. and Langridge, R., J. Mol. Graphics, 6 (1988) 13.
22. Cornell, W.D., Cieplak, P., Bayly, C.I., Gould, I.R., Merz, K.M., Ferguson, D.M., Spellmeyer, D.C., Fox, T., Caldwell, J.W. and Kollman, P.A., J. Am. Chem. Soc., 117 (1995) 5179.
23. Christensen, I.T. and Jorgensen, F.S., J Biomol Struct Dyn, 15 (1997) 473.
24. Fanelli, F., Menziani, C., Scheer, A., Cotecchia, S. and De Benedetti, P.G., Methods, 14 (1998) 302.
25. Sylte, I., Bronowska, A. and Dahl, S.G., Eur. J. Pharmacol., 416 (2001) 33.
26. Berman, H.M., Westbrook, J., Feng, Z., Gilliland, G., Bhat, T.N., Weissig, H., Shindyalov, I.N. and Bourne, P.E., Nucleic Acids Res., 28 (2000) 235.
27. Lin, Z., Wang, W., Kopajtic, T., Revay, R.S. and Uhl, G.R., Mol. Pharmacol., 56 (1999) 434.
28. Lin, Z., Itokawa, M. and Uhl, G.R., Faseb. J., 14 (2000) 715.
29. Kitayama, S., Shimada, S., Xu, H., Markham, L., Donovan, D.M. and Uhl, G.R., Proc. Natl. Acad. Sci. U S A, 89 (1992) 7782.
30. Kitayama, S., Wang, J.B. and Uhl, G.R., Synapse, 15 (1993) 58.
31. Kitayama, S., Morita, K., Dohi, T., Wang, J.B., Davis, S.C. and Uhl, G.R., Ann. N. Y. Acad. Sci., 801 (1996) 388.
32. Barker, E.L., Perlman, M.A., Adkins, E.M., Houlihan, W.J., Pristupa, Z.B., Niznik, H.B. and Blakely, R.D., J. Biol. Chem., 273 (1998) 19459.
33. Chen, J.G., Sachpatzidis, A. and Rudnick, G., J. Biol. Chem., 272 (1997) 28321.
34. Mitsuhata, C., Kitayama, S., Morita, K., Vandenbergh, D., Uhl, G.R. and Dohi, T., Brain Res. Mol. Brain Res., 56 (1998) 84.
35. Sur, C., Betz, H. and Schloss, P., Proc. Natl. Acad. Sci. U S A, 94 (1997) 7639.
36. Sur, C., Schloss, P. and Betz, H., Biochem. Biophys. Res. Commun., 241 (1997) 68.
37. Barker, E.L. and Blakely, R.D., Mol. Pharmacol., 50 (1996) 957.
38. Lee, S.H., Chang, M.Y., Lee, K.H., Park, B.S., Lee, Y.S. and Chin, H.R., Mol. Pharmacol., 57 (2000) 883.
39. Smicun, Y., Campbell, S.D., Chen, M.A., Gu, H. and Rudnick, G., J. Biol. Chem., 274 (1999) 36058.
40. Chen, J.G. and Rudnick, G., Proc. Natl. Acad. Sci. U S A, 97 (2000) 1044.
41. Bairoch, A. and Apweiler, R., Nucleic. Acids. Res., 27 (1999) 49.
42. Rost, B., Meth. Enzymol., 266 (1996) 525.
43. Kuroda, T., Shimamoto, T., Mizushima, T. and Tsuchiya, T., J. Bacteriol., 179 (1997) 7600.
44. Noumi, T., Inoue, H., Sakurai, T., Tsuchiya, T. and Kanazawa, H., J. Biochem. (Tokyo), 121 (1997) 661.
45. Inoue, H., Noumi, T., Tsuchiya, T. and Kanazawa, H., FEBS Lett., 363 (1995) 264.
46. Gerchman, Y., Olami, Y., Rimon, A., Taglicht, D., Schuldiner, S. and Padan, E., Proc. Natl. Acad. Sci. U S A, 90 (1993) 1212.
47. Gerchman, Y., Rimon, A. and Padan, E., J. Biol. Chem., 274 (1999) 24617.
48. Olami, Y., Rimon, A., Gerchman, Y., Rothman, A. and Padan, E., J. Biol. Chem., 272 (1997) 1761.
49. Rimon, A., Gerchman, Y., Kariv, Z. and Padan, E., J. Biol. Chem., 273 (1998) 26470.
50. Carroll, F.I., Gao, Y.G., Rahman, M.A., Abraham, P., Parham, K., Lewin, A.H., Boja, J.W. and Kuhar, M.J., J. Med. Chem., 34 (1991) 2719.
51. Pearson, W.R. and Lipman, D.J., Proc. Natl. Acad. Sci. USA, 85 (1988) 2444.
52. Loland, C.J., Norregaard, L. and Gether, U., J. Biol. Chem., 274 (1999) 36928.
53. Nicholls, A., Sharp, K.A. and Honig, B., Proteins, 11 (1991) 281.
54. Nicholls, A., *GRASP: Graphical Representation and Analysis of Surface Properties*, . 1992.
55. Chang, G. and Roth, C.B., Science, 293 (2001) 1793.
56. Murakami, S., Nakashima, R., Yamashita, E. and Yamaguchi, A., Nature, 419 (2002) 587.
57. Kawabe, T., Fujihira, E. and Yamaguchi, A., J. Biochem. (Tokyo), 128 (2000) 195.
58. Hirai, T., Heymann, J.A., Shi, D., Sarker, R., Maloney, P.C. and Subramaniam, S., Nat. Struct. Biol., 9 (2002) 597.
59. Bennett, E.R. and Kanner, B.I., J. Biol. Chem., 272 (1997) 1203.
60. Olivares, L., Aragon, C., Gimenez, C. and Zafra, F., J. Biol. Chem., 272 (1997) 1211.
61. Yu, N., Cao, Y., Mager, S. and Lester, H.A., FEBS Lett., 426 (1998) 174.
62. Hruz, P.W. and Mueckler, M.M., Biochemistry, 39 (2000) 9367.
63. Kleinberger-Doron, N. and Kanner, B.I., J. Biol. Chem., 269 (1994) 3063.
64. Larsen, N.A., Turner, J.M., Stevens, J., Rosser, S.J., Basran, A., Lerner, R.A., Bruce, N.C. and Wilson, I.A., Nat Struct Biol, 9 (2002) 17.
65. Rasmussen, S.G., Carroll, F.I., Maresch, M.J., Jensen, A.D., Tate, C.G. and Gether, U., J. Biol. Chem., 276 (2001) 4717.
66. Mortensen, O.V., Kristensen, A.S. and Wiborg, O., J. Neurochem., 79 (2001) 237.
67. Ferrer, J.V. and Javitch, J.A., Proc. Natl. Acad. Sci. USA, 95 (1998) 9238.
68. Loland, C.J., Norregaard, L., Litman, T. and Gether, U., Proc. Natl. Acad. Sci. USA, 99 (2002) 1683.
69. Fischer, J.F. and Cho, A.K., J. Pharmacol. Exp. Ther., 208 (1979) 203.
70. Liang, N.Y. and Rutledge, C.O., Biochem. Pharmacol., 31 (1982) 983.
71. Faivre, V., Manivet, P., Callaway, J.C., Airaksinen, M.M., Morimoto, H., Baszkin, A., Launay, J.M. and Rosilio, V., FEBS Lett., 471 (2000) 56.
72. Chen, N., Ferrer, J.V., Javitch, J.A. and Justice, J.B., Jr., J. Biol. Chem., 275 (2000) 1608.
73. Reith, M.E., Berfield, J.L., Wang, L.C., Ferrer, J.V. and Javitch, J.A., J. Biol. Chem., 276 (2001) 29012.
74. Schmid, J.A., Scholze, P., Kudlacek, O., Freissmuth, M., Singer, E.A. and Sitte, H.H., J. Biol. Chem., 276 (2001) 3805.
75. Kilic, F. and Rudnick, G., Proc. Natl. Acad. Sci. USA, 97 (2000) 3106.

76. Hastrup, H., Karlin, A. and Javitch, J.A., Proc. Natl. Acad. Sci. USA, 98 (2001) 10055.
77. Chang, A.S., Starnes, D.M. and Chang, S.M., Biochem. Biophys. Res. Commun., 249 (1998) 416.
78. Thompson, J.D., Higgins, D.G. and Gibson, T.J., Nucleic Acids Res., 22 (1994) 4673.